Dermatology Practical & Conceptual

Dermoscopic Features of Cutaneous Vasculitis

Ozge Sevil Karstarli Bakay[1], Nida Kacar[1], Melis Gonulal[2], Nese Calli Demirkan[3], Hülya Cenk[1], Sule Goksin[1], Yunus Gural[4]

1 Pamukkale University Faculty of Medicine, Department of Dermatology, Denizli, Turkey
2 Tepecik Education and Research Hospital Department of Dermatology, University of Health Sciences Turkey, İzmir, Turkey
3 Department of Pathology, Medical Faculty, Pamukkale University, Denizli, Turkey
4 Firat University Faculty of Science, Division of Statistics, Elazig, Turkey

Key words: Dermoscopy, machine learning, cutaneous vasculitis, inflammoscopy

Citation: Karstarli Bakay OS, Kacar N, Gonulal M, et al. Dermoscopic Features of Cutaneous Vasculitis. *Dermatol Pract Concept.* 2024;14(1):e2024051. DOI: https://doi.org/10.5826/dpc.1401a51

Accepted: August 26, 2023; **Published:** January 2024

Funding: None.

Competing Interests: None.

Authorship: All authors have contributed significantly to this publication.

Corresponding Author: Ozge Sevil Karstarli Bakay, Pamukkale University, Faculty of Medicine, Department of Dermatology, 20160, Kınıklı Campus. Denizli, Turkey. Phone: +095376755441 E-mail: ozgekarstarli@hotmail.com

ABSTRACT

Introduction: Dermoscopy has become widespread in the diagnosis of inflammatory skin diseases. Cutaneous vasculitis (CV) is characterized by inflammation of vessels, and a rapid and reliable technique is required for the diagnosis.

Objectives: We aimed to define CV dermoscopic features and increase the diagnostic accuracy of dermoscopy with machine learning (ML) methods.

Methods: Eighty-nine patients with clinically suspected CV were included in the study. Dermoscopic images were obtained before biopsy using a polarized dermoscopy. Dermoscopic images were independently evaluated, and interobserver variability was calculated. Decision Tree, Random Forest, and K-Nearest Neighbors were used as ML classification models.

Results: The histopathological diagnosis of 58 patients was CV. Three patterns were observed: homogeneous pattern, mottled pattern, and meshy pattern. There was a significant difference in background color between the CV and non-CV groups ($P = 0.001$). The milky red and livedoid background color were specific markers in the differential diagnosis of CV (sensitivity 56.7%, specificity 96.3%, sensitivity 29.4%, specificity 99.2%, respectively). Red blotches were significantly more common in CV lesions ($P = 0.038$). Red dots, comma vessels, and scales were more common in the non-CV group ($P = 0.002$, $P = 0.002$, $P = 0.003$, respectively). Interobserver agreement was very good for both pattern ($\kappa = 0.869$) and background color analysis ($\kappa = 0.846$) ($P < 0.001$). According to ML classifiers, the background color and lack of scales were the most significant dermoscopic aspects of CV.

Conclusions: Dermoscopy may guide as a rapid and reliable technique in CV diagnosis. High accuracy rates obtained with ML methods may increase the success of dermoscopy.

Introduction

Vasculitis is defined as blood vessel wall inflammation and can affect small, medium, or large vessels. Clinical manifestations occur depending on the size of the affected vessels, involving many organ systems in the body [1]. The most common form of cutaneous vasculitis (CV) is cutaneous small-vessel vasculitis (CSVV). CSVV affects small vessels in the superficial and middle dermis of the skin, including arterioles, capillaries, and postcapillary venules [1,2]. CSVV typically presents with palpable or macular purpura, but urticarial papules, pustules, blisters, petechiae, or targetoid lesions may be seen [1].

Skin biopsy remains the gold standard for diagnosis, classification, and exclusion of imitators in CV. The term leukocytoclastic vasculitis (LCV) refers to the histopathological description of a common form of CSVV [2]. Classical histopathological findings of LCV are neutrophilic infiltration with signs of leukocytoclasia, fibrinoid necrosis, extravasated red blood cells, and damaged endothelial cells. Histopathologically, LCV can be found in ANCA-associated vasculitis, immunocomplex vasculitis such as IgA vasculitis (Henoch–Schonlein purpura), urticarial vasculitis, and vasculitis-related systemic diseases [3].

In patients with CV, radiological and laboratory evaluations should be performed to investigate systemic involvement [4]. Since histopathological diagnosis takes time, many patients with clinical suspicion of CV are exposed to unnecessary laboratory examinations or immunosuppressive therapies. Therefore, there is a need for a rapid and reliable diagnostic tool that will reduce unnecessary evaluations and invasive procedures.

A dermatoscope is an optical device that allows visualization of the epidermis, dermo-epidermal junction, and papillary dermis, which cannot be seen with the naked eye. Few studies with small groups have suggested that dermoscopy can be used as a rapid and noninvasive method for the diagnosis of CV [5-9].

The correct diagnosis rate of both pigmented and non-pigmented lesions with dermoscopic examination is higher than the unaided eye [10,11]. However, dermoscopy requires special training and experience. Manual review of dermoscopy images, even by well-trained dermatologists, is often time-consuming and subjective. There is increasing research on the development of artificial intelligence (AI) techniques to minimize diagnostic errors due to the difficulty and subjectivity of visual interpretation [12,13]. The field of AI includes machine learning (ML) and its subset, deep learning (DL) techniques, which use complex algorithms to build models that can make these predictions [14].

Objectives

We aimed to investigate the dermoscopic findings of CV. In addition, we analyzed dermatoscopic findings using the ML method to improve the accuracy of dermoscopic diagnosis of vasculitis.

Methods

This prospective study was conducted at Pamukkale University and included patients with clinically suspected CV. The procedures of the clinical photograph, dermoscopic examination, and skin biopsy had been performed after the informed consent of the patients and were conducted following the Helsinki Declaration. The study was approved by the Ethics Committee of the Pamukkale University Training and Research Hospital, Denizli, Turkey. Individuals over the age of 18 years with macular or papular purpuric lesions were included in the study. A 4-mm punch biopsy was taken from palpable purpura that emerged within 24-48 hours. Biopsy was taken from all patients for definitive diagnosis. Dermoscopic examination preceded biopsy, and both were performed on the same lesions. It was planned to include patients presenting within 3 years of local ethics committee approval. The dermoscopic images of each lesion were taken using a polarized dermoscopy (DermLite Foto, ×10 magnification; 3Gen) adopted on a digital camera (Canon G10; Canon). Among 99 patients with purpuric lesions, we excluded ten patients who did not have a definite histopathological diagnosis or clear dermoscopic image records. A checklist was created based on a review of articles on dermoscopic examination of purpuric lesions and all images were assessed by a dermatologist (NK) experienced in dermoscopy [5,15-19]. Three dermatologists (OSKB, HC, SG) independently evaluated the pattern and background of the dermoscopic images, and interobserver agreement was calculated. All authors evaluating dermoscopic images were blind to histopathological diagnosis.

Statistical Analysis

Statistical package program SPSS 22.0 was used in the analysis of the data. The interobserver agreement was determined using Fleiss Kappa statistics. The relationship between disease groups (CV and non-CV) and dermoscopic findings was evaluated using Cramer's V statistics. The frequency, sensitivity, and specificity of dermoscopic features found in cutaneous vasculitis were calculated.

Decision Tree, Random Forest (RF), and K-nearest neighbors (KNN) were used as classification models for machine learning. The dermoscopic features were input as independent variables, while the main disease groups (CV and non-CV) were used as dependent variables. Decision tree analysis is a predictive modeling tool that can be applied in many areas and uses a branching structure to show the consequences of a decision. Decision trees can be created with an algorithmic approach that can split the data set in different ways according to different conditions. Decisions

are the most powerful algorithms that fall under the category of supervised algorithms. It can be used to map the possible consequences of a decision. Each node represents a possible outcome [20]. RF is a decision tree-based ensemble learning method. It follows an algorithm that uses a bootstrap resampling technique to select samples repeatedly randomly from the original training sample set as the training set and the remaining samples as the test set [21]. KNN is a non-parametric classification method that collects existing classes and then classifies the new classes according to the comparison measure [15]. All dermoscopic features were run through machine learning classifiers to assess the accuracy of CV diagnosis. We take 80% of the patients as the training set and 20% of the patients as the validation set. The classifiers performance was assessed using accuracy, precision, sensitivity, and specificity.

Results

Histopathological diagnoses of 89 patients (42 women; 47 men) were CV in 58 patients, including LCV in 48 patients, Henoch-Schönlein purpura in 9 patients, and urticarial vasculitis in 1 patient. In the histopathological diagnosis of the remaining 31 patients, pigmented purpuric dermatosis (PPD) was the most prevalent diagnosis with 14 patients, the others were 10 chronic dermatitis (CD), 2 lichen planus, 2 mycosis fungoides, 1 erythema multiforme, 1 folliculitis and 1 pseudoxanthoma elasticum.

The most significant histological signs of LCV were the deposition of fibrin in the vessel walls and perivascular polymorphonuclear leukocytes in the upper or middle dermis.

Three patterns were observed according to the arrangement of the vessels; 1) structureless purpuric area, termed as homogeneous, 2) multiple erythematous and/or bluish blotches and/or globules and/or dots arranged uniformly over a structureless background, termed as mottled and 3) consists of a vascular network, we termed as reticular (Figure 1). Mottled pattern was commonly detected in both groups (Table 1). The total kappa value was 0.869 (Table 2) in the evaluation of the dermoscopic images of the three dermatologists in terms of pattern, representing very good agreement ($P < 0.001$).

Three background colors were observed: yellowish-erythematous, milky-red, and livedoid. There was a significant difference in background color between the CV and non-CV groups ($P = 0.001$). The yellowish erythematous background color was detected in 80.6% of the non-CV group. The milky red (sensitivity 56.7%, specificity 96.3%) and livedoid background color (sensitivity 29.4%, specificity 99.2%) was found as specific markers in the differential diagnosis of CV lesions, showing low sensitivity. Interobserver agreement was also very good for background color analysis (Table 2) ($\kappa = 0.846$, $P < 0.001$).

The most common dermoscopic finding in CV was red globules (N = 43, 74.1%). Red blotches were detected in 26 (44.8%) CV lesions, but it was seen in only 7 (22.6%) lesions in the non-CV group, and this difference was statistically significant ($P = 0.038$; sensitivity 78.8%, specificity 42.9%) (Table 1).

The rate of presence of red dots, comma vessels, and scales in CV lesions was very low compared to the non-CV group and this difference was statistically significant (Table 1) ($P = 0.002$, $P = 0.002$, $P = 0.003$, respectively).

Remarkably, none of the PPD lesions had blue-gray background color. milky red and blue-gray background color were specific markers for CV ($P = 0.002$, sensitivity 56.7%, specificity 99.8% and sensitivity 29.4%, specificity 100%, respectively). Similar to CV, the most common dermoscopic finding in PPD was red globules (N = 13, 92.8%). Red dots (64.28%), comma (50%), and annular (57.1%) vessels were more common in PPD ($P < 0.01$).

There was no correlation between dermoscopic patterns and histopathological findings such as erythrocyte extravasation, the presence of fibrinogen, and eosinophil. Erythrocyte extravasation was observed more frequently in lesions with a yellowish erythematous background color. The relationship

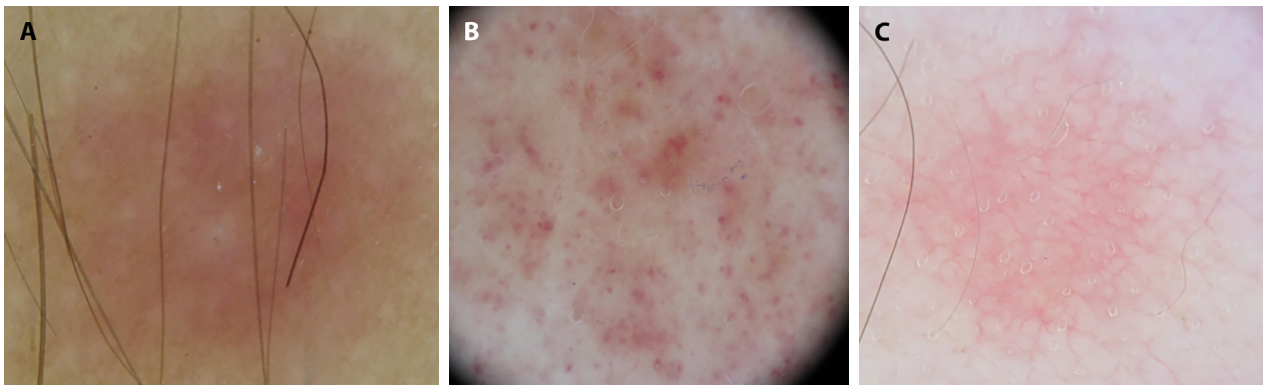

Figure 1. Dermoscopic patterns of purpuric lesions. (A) Homogeneous pattern: structureless purpuric area. (B) Mottled pattern: multiple erythematous and/or bluish blotches and/or globules and/or dots arranged uniformly over a structureless background. (C) Reticular pattern: branched vessels of which branches were arranged in a meshy configuration over a structureless background.

Table 1. Dermoscopic findings observed in purpuric lesions.

		CV N (%)	Non-CV N (%)	Cramer V	P value
Pattern	Homogeneous	16 (28.1)	9 (29)	0.190	0.524
	Mottled	38 (66.7)	19 (63.3)		
	Meshy	3 (5.3)	3 (9.7)		
Background color	Yellowish Erythematous	23 (39.7)	25 (80.6)	0.392	0.001
	Milky-red	25 (43.1)	4 (12.9)		
	Blue-gray	10 (17.2)	2 (6.5)		
Linear vessels		17 (29.3)	8 (25.8)	0.037	0.726
Red dots		16 (27.6)	19 (61.3)	0.329	0.002
Red globules		43 (74.1)	23 (74.2)	0.001	0.995
Red blotches		26 (44.8)	7 (22.6)	0.219	0.038
Blue globules		8 (13.8)	5 (16.1)	0.032	0.766
Annular vessels		8 (13.8)	8 (25.8)	0.149	0.160
Comma vessels		5 (8.6)	11 (35.5)	0.333	0.002
Scale		8 (13.8)	13 (41.9)	0.316	0.003
Branched vessels		13 (22.4)	3 (9.7)	0.158	0.136

Table 2. Fleiss kappa analysis to assess the interobserver agreement of dermoscopic patterns and background colors in purpuric lesions.

	Agreement on Individual Categories			Overall Agreement	
	Rating Category	Fleiss Kappa	P	Fleiss Kappa	P
Patern	Homojen	0.900	<0.001	0.869	<0.001
	Mottled	0.935	<0.001		
	Reticular	0.703	<0.001		
Background color	Yellowish-erythematous	0.865	<0.001	0.846	<0.001
	Milky red	0.869	<0.001		
	Blue-gray	0.769	<0.001		

Table 3. Machine learning classifier performance measures.

	Accuracy	Precision (Positive Predictive Value)	Sensitivity (%)	Specificity (%)
RF	0.882	0.882	0.882	0.871
Decision Tree	0.824	0.824	0.802	0.631
KNN	0.706	0.690	0.706	0.617

KNN = K-nearest neighbors; RF = Random Forest.

between erythrocyte extravasation and background color was statistically significant (Cramer V=0.275, P = 0.009).

RF, Decision Tree, and KNN give classification rates of 88.0%, 82.40%, and 70.6% accuracy, respectively. The highest accuracy, precision, sensitivity, and specificity values were achieved with RF classification (Table 3).

The three dermoscopic findings with the highest importance score in the diagnosis of CV according to RF classification were scale, background color, and red dots, respectively. Decision Tree classification presented an algorithm using 80% of samples for training data and 20% of samples for validation data (Figure 2).

Conclusions

Dermoscopic identification of vascular lesions may guide patient management. Most vascular proliferative lesions have well-defined, variable-colored areas called lacunae on dermoscopy [22]. In addition to proliferative vascular lesions, dermoscopic features of inflammatory vascular lesions are a matter of interest. Pigmented purpuric dermatoses (PPDs) are a group of inflammatory skin diseases that may be mistaken as vasculitides [23]. Common dermoscopic characteristics of PPDs include a copper-red background, rounded

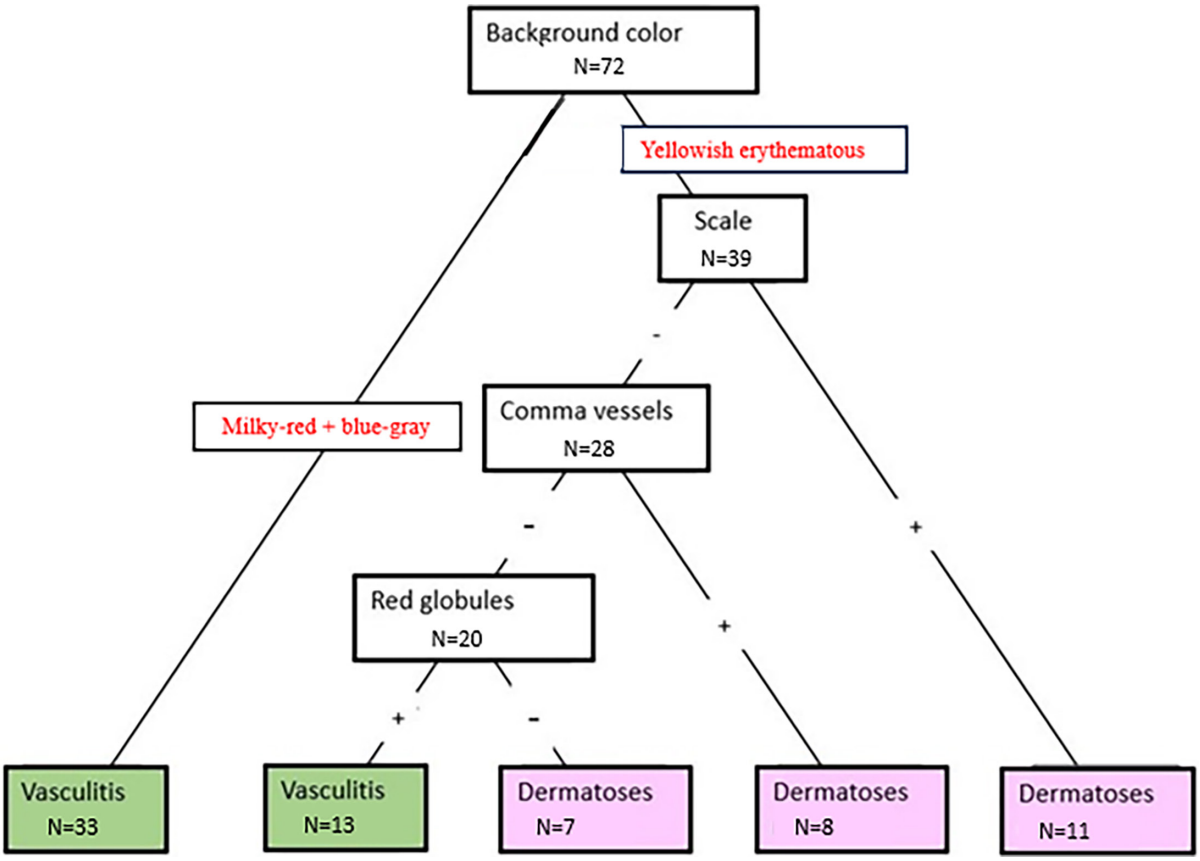

Figure 2. Decision Tree Plot: decision tree classification presented an algorithm using 17 samples for training data and 72 samples for validation data. By following this algorithm, Decision Tree predicted cutaneous vasculitis diagnosis with approximately 80% accuracy.

to oval dots, gray dots, and a network of brownish-to-gray linked lines [22].

Four basic dermoscopic patterns have been reported for purpuric lesions including homogeneous, mottled, perifollicular, and epidermal purpuric by Vazquez-Lopez et al. The homogeneous pattern has been suggested to characterize a noninflammatory form of purpura, such as bleeding diathesis, presenting with wide, homogeneous, structureless purpuric areas; while the mottled pattern, consisting of multiple small, speckled, blurred purpuric blotches and/or globules over a purple to the orange-brown background, to characterize an inflammatory form, such as LCV and PPD [17]. In the present study, the most common pattern was the mottled pattern. However, the homogeneous pattern was detected in a significant part of the inflammatory disease lesions. With these results, we concluded that the homogeneous pattern not only characterizes the non-inflammatory form of purpura but can also be seen in inflammatory skin diseases. Although purpura, the most common manifestation of cutaneous vasculitis, is highlighted by dermoscopy, there is little evidence of the dermoscopic pattern of diseases included in this group [17,18].

In the literature, most of the studies on dermoscopic findings of cutaneous vasculitis focused on the differential diagnosis of common urticaria and urticarial vasculitis [5,6,9]. On the other hand, purpuric dots or globules on an orange-brown background have been suggested as an important dermoscopic finding for urticarial vasculitis [6 9].

In the study of Choo et al, which included 15 true vasculitis and 15 vasculopathy cases, found the mottled pattern and orange-brown background most frequently in both groups. The term vasculopathy is used to describe conditions with significant histopathological vascular changes that do not fully meet the criteria for vasculitis [24]. The most common vasculopathy detected in this study was PPD (N = 14). The subgroups of PPDs observed in our patients included progressive pigmentary dermatosis (Schamberg disease) and lichen aureus. They reported that blue-gray blotches were found only in the vasculitis group and an important finding for differentiation [7]. In our study, there were 58 patients with true vasculitis and 14 patients with vasculopathy (PPD). Similarly, we found the most common mottled pattern in both groups and yellowish erythematous background color in PPD. The yellowish erythematous background of PPD is related to the presence of a dense lymphocytic and histiocytic infiltrate in the dermis caused by the extravasation of red blood cells and the presence of hemosiderin in histiocytes [16]. Unlike the study of Choo et al, the most common background color in CV lesions in our study was milky red. This difference is most likely due to the age of

the vasculitis lesions. Differences in background color reflect the status of extravasated erythrocytes. Intact erythrocytes reflect a purplish color while siderophages reflect a yellowish color [17]. Milk red background color is more likely in the early period, however, the probability of encountering an orange-brown color increases in the late period. Similarly, in our study, blue-gray background color (Figure 3) was only present in cases of true vasculitis, and this difference was statistically significant. Necrotic lesions are seen by dermoscopy as whitish-blue patches [17]. Probably because necrosis is not expected in vasculopathy, bluish-gray patches are not observed in dermoscopy. In the present study, red globules were the most common finding in both CV and PPD, whereas red dots, annular and comma vessels were significantly more common in PPD. Red globules in dermoscopy of LCV are reflections of extravasated erythrocytes secondary to fibrinoid degeneration of small vessel walls. However, the red globules of PPD are associated with variable amounts of erythrocytes, lymphocytes, and siderophages surrounding swollen blood vessels in the upper dermis [17]. Presumably, these swollen blood vessels seem as comma or annular vessels on dermoscopy. We suggest that, since it is difficult to see intact vascular structures in CV, most likely due to fibrinoid degeneration, comma/annular vessels are few and the red blotches that we detect quite frequently in CV (44.8%) reflect fragmented vascular structures.

Dotted vessels in a patchy distribution on a dull red background and yellow scales have been identified as CD most common dermoscopic features [25]. In our study, scales, dotted and comma vessels were significantly more common in the dermatoses group and were important dermoscopic findings in differentiating from CV.

Remarkably, in addition to the four patterns that had previously been identified on dermoscopy of purpuric lesions, we additionally observed the 'reticular pattern', which is composed of reticular dilated vessels (Figure1C).

In the present study, interobserver agreement was quite high in terms of background color and pattern. This was evidence of the reliability and validity of these dermoscopic findings. We also evaluated dermoscopic data with RF, Decision Tree, and KNN, which are the mostly used ML classification methods [26]. We achieved over 80% accurate diagnosis of CV with RF (88%) and Decision Tree (82%). The sensitivity, specificity, and positive predictive value of the RF classifier were also above 80% (Table 3). Although studies that evaluate dermoscopic images with AI mostly focus on melanoma, there are also studies on different diseases such as non-melanoma skin cancers, onychomycosis, and rosacea. [13,27-29]. In our literature review, no study was found in which vasculitis dermoscopy was combined with AI. However, there were studies in which the dermoscopy of vascular structures, which has an important place in vasculitis dermoscopy, was evaluated with AI [26,30]. In our study, RF and decision tree classifiers, which are ML methods, highlighted background color, scales, red dots, and comma vessels as distinctive dermoscopic findings in the classification of purpuric lesions.

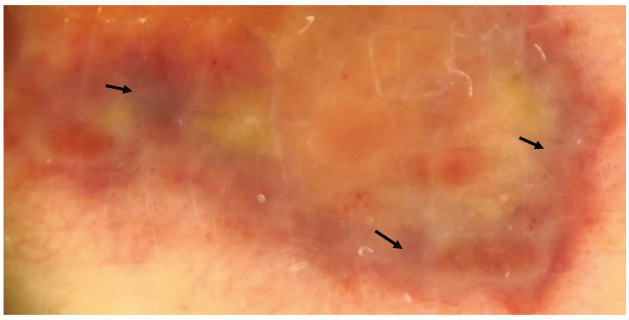

Figure 3. Blue-gray background color in cutaneous vasculitis: blue gray patches (black arrows) were detected as a highly specific dermoscopic finding for cutaneous vasculitis.

The relatively small number of samples is a limitation of this study. However, its strengths are that it is one of the few studies in the literature in which dermoscopic data of cutaneous vasculitis is examined and that interobserver agreement has been evaluated.

In conclusion, although the histopathological examination is the gold standard in the diagnosis of cutaneous vasculitis, the evaluation of patients with dermoscopy in the first step seems valuable for patient management. Red globules and blotches in a mottled distribution on a milky-red background without scales were the most frequent dermoscopic features for CV.

References

1. Wette DA, Dutz JP, Shinkai K, Fox LP. Cutaneous Vasculitis. In: *Dermatology* (Bolognia JL, Schaffer JV, Cerroni Lorenzo, eds), 4th edn. China: Elsevier Ltd.,2018: 409-439.
2. Antonov D, Kamarashev J, Kazandjieva J, Neykova T, Tsankov N. The rash that becomes purpuric, petechial, hemorrhagic, or ecchymotic. *Clin Dermatol.* 2020;38(1):3-18. DOI: 10.1016/j.clindermatol.2019.07.036. PMID: 32197746.
3. Fraticelli P, Benfaremo D, Gabrielli A. Diagnosis and management of leukocytoclastic vasculitis. *Intern Emerg Med.* 2021;16(4):831-841. DOI: 10.1007/s11739-021-02688-x. E PMID: 33713282. PMCID: PMC8195763.
4. Elbendary A, Abdel-Halim MRE, Ragab G. Updates in cutaneous manifestations of systemic vasculitis. *Curr Opin Rheumatol.* 2022;34(1):25-32. DOI: 10.1097/BOR.0000000000000847. PMID: 34690279.
5. Vázquez-López F, Fueyo A, Sánchez-Martín J, Pérez-Oliva N. Dermoscopy for the screening of common urticaria and urticaria vasculitis. *Arch Dermatol.* 2008;144(4):568. V DOI: 10.1001/archderm.144.4.568. PMID: 18427065.
6. Suh KS, Kang DY, Lee KH, et al. Evolution of urticarial vasculitis: a clinical, dermoscopic and histopathological study. *J Eur Acad Dermatol Venereol.* 2014;28(5):674-675. DOI: 10.1111/jdv.12263. PMID: 23998438.

7. Choo JY, Bae JM, Lee JH, Lee JY, Park YM. Blue-gray blotch: A helpful dermoscopic finding in optimal biopsy site selection for true vasculitis. *J Am Acad Dermatol*. 2016;75(4):836-838. C DOI: 10.1016/j.jaad.2016.05.022. PMID: 27646743.
8. Quijano-Gomero EG, Rodríguez-Zúñiga MJM, Sanz-Montero ME, Durand-Buse D. Clinical, Dermoscopic and Histologic Features of Recurrent Cutaneous Eosinophilic Vasculitis Cases. *Actas Dermosifiliogr (Engl Ed)*. 2019;110(7):590-596. DOI: 10.1016/j.ad.2017.12.012. PMID: 29937063.
9. García-García B, Aubán-Pariente J, Munguía-Calzada P, Vivanco B, Argenziano G, Vázquez-López F. Development of a clinical-dermoscopic model for the diagnosis of urticarial vasculitis. *Sci Rep*. 2020;10(1):6092. DOI: 10.1038/s41598-020-63146-w. PMID: 32269296. PMCID: PMC7142109.
10. Rosendahl C, Tschandl P, Cameron A, Kittler H. Diagnostic accuracy of dermatoscopy for melanocytic and nonmelanocytic pigmented lesions. *J Am Acad Dermatol*. 2011;64(6):1068-1073. DOI: 10.1016/j.jaad.2010.03.039. PMID: 21440329.
11. Sinz C, Tschandl P, Rosendahl C, et al. Accuracy of dermatoscopy for the diagnosis of nonpigmented cancers of the skin. *J Am Acad Dermatol*. 2017;77(6):1100-1109. DOI: 10.1016/j.jaad.2017.07.022. PMID: 28941871.
12. Seeja RD, Suresh A. Deep Learning Based Skin Lesion Segmentation and Classification of Melanoma Using Support Vector Machine (SVM). *Asian Pac J Cancer Prev*. 2019;20(5):1555-1561. DOI: 10.31557/APJCP.2019.20.5.1555. PMID: 31128062. PMCID: PMC6857898.
13. Tschandl P, Rosendahl C, Akay BN, Aet al. Expert-Level Diagnosis of Nonpigmented Skin Cancer by Combined Convolutional Neural Networks. *JAMA Dermatol*. 2019;155(1):58-65. DOI: 10.1001/jamadermatol.2018.4378. PMID: 30484822. PMCID: PMC6439580.
14. Murphree DH, Puri P, Shamim H, et al. Deep learning for dermatologists: Part I. Fundamental concepts. *J Am Acad Dermatol*. 2022;87(6):1343-1351. DOI: 10.1016/j.jaad.2020.05.056. PMID: 32434009. PMCID: PMC7669702.
15. DG Stork, RO Duda, PE Hart, D Stork. Pattern Classification. 2001 Wiley: Hoboken, NJ, USA.
16. Martín JM, Bella-Navarro R, Jordá E. Vascularización en dermatoscopia [Vascular patterns in dermoscopy]. *Actas Dermosifiliogr*. 2012;103(5):357-75. DOI: 10.1016/j.ad.2011.11.005. PMID: 22463770.
17. Vazquez-Lopez F, García-García B, Sanchez-Martin J, Argenziano G. Dermoscopic patterns of purpuric lesions. *Arch Dermatol*. 2010;146(8):938. DOI: 10.1001/archdermatol.2010.162. PMID: 20713845.
18. Sgouros D, Apalla Z, Ioannides D, et al. Dermoscopy of Common Inflammatory Disorders. *Dermatol Clin*. 2018;36(4):359-368. Sgouros D, Apalla Z, Ioannides D, Katoulis A, Rigopoulos D, Sotiriou E, Stratigos A, Vakirlis E, Lallas A. Dermoscopy of Common Inflammatory Disorders. *Dermatol Clin*. 2018;36(4):359-368. DOI: 10.1016/j.det.2018.05.003. PMID: 30201145.
19. Errichetti E. Dermoscopy in general dermatology (non-neoplastic dermatoses): pitfalls and tips. *Int J Dermatol*. 2021;60(6):653-660. DOI: 10.1111/ijd.15427. PMID: 33533022.
20. Song YY, Lu Y. Decision tree methods: applications for classification and prediction. *Shanghai Arch Psychiatry*. 2015;27:130–135. DOI: 10.11919/j.issn.1002-0829.215044. PMID: 26120265. PMCID: PMC4466856.
21. Breiman L. Random forests. Machine Learning 2001;45(1):5-32.
22. Piccolo V, Russo T, Moscarella E, Brancaccio G, Alfano R, Argenziano G. Dermatoscopy of Vascular Lesions. *Dermatol Clin*. 2018;36(4):389-395. DOI: 10.1016/j.det.2018.05.006. PMID: 30201148.
23. Karstarlı Bakay OS, Bakay U. A case of certolizumab-induced purpura annularis telangiectodes of Majocchi and literature review. *Int J Rheum Dis*. 2023 Jul 31. DOI: 10.1111/1756-185X.14854. PMID: 37522716.
24. Barnhill RL, Nousari CH, Xu X, Barksdale SK. Vascular diseases. *Lever's histopathology of the skin*. 2009. Eds: Elder DE Elenitsas R, Johnson BL, Murphy GF, Xu X. Wolters Kluwer/Lippincott Williams-Wilkins London, Philadelphia:205-324.
25. Xu C, Liu J, Wang T, Luo Y, Liu Y. Dermoscopic patterns of early-stage mycosis fungoides in a Chinese population. *Clin Exp Dermatol*. 2019;44(2):169-175. DOI: 10.1111/ced.13680. PMID: 29876963.
26. Kharazmi P, Zheng J, Lui H, Jane Wang Z, Lee TK. A Computer-Aided Decision Support System for Detection and Localization of Cutaneous Vasculature in Dermoscopy Images Via Deep Feature Learning. *J Med Syst*. 2018;42(2):33. DOI: 10.1007/s10916-017-0885-2. PMID: 29318397.
27. Sharma AN, Shwe S, Mesinkovska NA. Current state of machine learning for non-melanoma skin cancer. *Arch Dermatol Res*. 2022;314(4):325-327. DOI: 10.1007/s00403-021-02236-9. PMID: 33991230.
28. Zhu X, Zheng B, Cai W, et al. Deep learning-based diagnosis models for onychomycosis in dermoscopy. *Mycoses*. 2022;65(4):466-472. Z DOI: 10.1111/myc.13427. PMID: 35119144.
29. Ge L, Li Y, Wu Y, Fan Z, Song Z. Differential Diagnosis of Rosacea Using Machine Learning and Dermoscopy. *Clin Cosmet Investig Dermatol*. 2022;15:1465-1473. DOI: 10.2147/CCID.S373534. PMID: 35935599. PMCID: PMC9354760.
30. Jaworek-Korjakowska J. A Deep Learning Approach to Vascular Structure Segmentation in Dermoscopy Colour Images. *Biomed Res Int*. 2018;2018:5049390. DOI: 10.1155/2018/5049390. PMID: 30515404. PMCID: PMC6236870.